The Ballooning of Outflows

Doron Nof*

Department of Oceanography, The Florida State University, Tallahassee, Florida

Thierry Pichevin

EPSHOM/CMO, Brest, France

ABSTRACT

It has been recently shown that when an inviscid outflow empties into the ocean, a *steady* alongshore current (in the Kelvin wave sense) cannot be established. This is due to the impossibility of balancing the alongshore momentum flux. To offset this momentum-flux deficit the outflow balloons near its source, forming an anticyclonic bulge. Using 1½-layer analytical and numerical models, the authors show that, on an *f* plane, the Coriolis force associated with the offshore movement of the growing bulge (which pushes itself away from the wall) compensates for the momentum flux of the longshore current downstream. With the aid of the slowly varying approximation, an inviscid nonlinear analytical solution is constructed. Numerical simulations with the Bleck and Boudra model are also performed.

It is found that an outflow with an intense anticyclonic vorticity (i.e., a zero potential vorticity outflow with a relative vorticity of $-f$) produces a steep gyre that balloons (i.e., its radius increases with time) quickly at the rate of $8g'Q/3\pi f^2 R^3$ (where g' is the reduced gravity, Q is the outflow's discharge, f the Coriolis parameter, and R is the instantaneous bulge radius). Such an intense (large Rossby number) outflow dumps most of its mass flux (66%) into the growing bulge rather than into the longshore current downstream (which receives the remaining 33% of the total flux). An outflow with a weakly anticyclonic vorticity ($-\alpha f$, where α is analogous to the Rossby number and is much smaller than unity), on the other hand, dumps most of its water [$(1 - 2\alpha)Q$] into the downstream current rather than into the bulge. Even though less mass flux is going into the bulge in this weak vorticity case, the bulge balloons at a somewhat faster rate ($4g'Q/\pi f^2 R^3$) than the intense outflow does because the bulge is now relatively flat so that most of the incoming water goes toward an increase in size rather than toward an increase in thickness.

Numerical simulations are in good agreement with the above analytical solutions. They show that frictional forces increase the downstream current mass flux. The simulations also show that friction very gradually alters the potential vorticity of the bulge. Applications to the initial growing stage of Loop Current rings (which constitute an "outflow bulge" in the sense that it corresponds to water flowing from the Caribbean into the Gulf of Mexico), to rivers outflow, to bulges of plumes in other numerical models, and to bulges in laboratory outflows are discussed.

1. Introduction

The manner in which water of anomalous density empties into an ocean has been of interest to oceanographers for decades. In particular, various attempts have been made to understand how the anomalous water is distributed once it debouches into the ocean. In everyday life, a source of anomalous water emptying into a large container tends to spread evenly in all directions. In the

ocean, however, the earth's rotation tends to confine the outflow to the coast (in the Kelvin wave sense) forming an alongshore current. The complications added by (uniform) rotation do not end here, and recent analytical and numerical studies have shown that such an (inviscid) outflowing current is unsteady [see Fig. 1 and Pichevin and Nof (1997, hereafter PN)]. Furthermore, numerical simulations demonstrate that, on an *f* plane, the outflow balloons in the sense that a growing bulge is generated near the coast (PN; Fong 1998). Here, we present the first nonlinear analytical solution for the growth rate of the bulge on an *f* plane. We also present numerical simulations, which confirm our analytical calculations.

a. Observational background

There are many situations where water of one density enters an oceanic basin with a different density. The

---

* Additional affiliation: The Geophysical Fluid Dynamics Institute, The Florida State University, Tallahassee, Florida.

Corresponding author address: Dr. Doron Nof, Dept. of Oceanography 4320, The Florida State University, Tallahassee, FL 32306-4320.
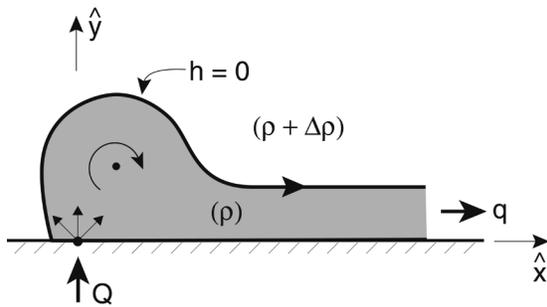E-mail: nof@ocean.fsu.edu

FIG. 1. A schematic diagram of the steady configuration shown by Pichevin and Nof (1997) to be impossible. In the PN scenario, a steady inviscid outflow cannot exist because the alongshore momentum flux of the downstream current is not balanced. As a result of this impossibility, the bulge grows forever and the downstream current mass flux is smaller than the incoming mass flux Q (see Fig. 2).

largest one is probably that of the Yucatan Strait through which about 20–30 Sv (Sv $\equiv 10^6$ m^3 s^{-1}) of warm Caribbean water enters the cooler Gulf of Mexico (see, e.g., Sturges 1994) and forms a gyre 3–4 times the width of the downstream current. Going down in scale, the surface flows through the Tsugaru and the Gibraltar straits (approximately 1 Sv) exhibit similar characteristics (Nof and Pichevin 1999) and form gyres as much as 10 times the size of the downstream currents. Still smaller (<1 Sv) are the well-studied outflows from the Mississippi River, Chesapeake Bay, and the Niagara River [see, e.g., Boicourt 1973; Bowman 1978; Drinkwater 1988; Masse and Murthy 1992; Horner et al. 2000; Atkinson and Wallace 1975 (where evidence for the presence of Mississippi water east of the outflow is presented)]. In contrast to the large and moderate outflows, which form large ballooning bulges, these smaller outflows form *modest* gyres, which are, at the most, twice the size of the downstream currents.

b. Modeling background

As pointed out by Yankovsky and Chapman (1997), there are mainly two kinds of outflows with two different kinds of dynamics. The first kind is "surface trapped" (in the sense that it does not feel the bottom) whereas the second is "bottom trapped" (in the sense that it is dominated by bottom topography). We shall focus here on the first kind of outflow.

Until fairly recently, it has been believed that, on an f plane, such surface-trapped outflows can always reach a steady state. However, as has just been pointed out, PN have shown, analytically and numerically, that a steady state cannot be reached due to the impossibility of balancing the alongshore momentum flux. The same conclusions were later reached by Fong (1998) using three-dimensional numerical simulation and by Horner et al. (2000) using laboratory experiments on a rotating table. Note, however, that when Horner et al. (2000) reduced the angle between the axis of the outflow and the coast from 90° (corresponding to the PN case) to

35°–55°, a steady state (with a modest gyre) was reached. (Why this is so will become clear shortly.)

As far as specific outflows are concerned, the exchange via the Yucatan Strait was examined by Hurlburt and Thompson (1980) and PN. Both of these studies have shown that, in this case, the bulge formed by the outflow (from the Caribbean into the Gulf of Mexico) is so great that β is important to the process. This is also the case with the surface flows through the Tsugaru and Gibraltar straits, which form gyres on the scale of $O(100$ km). On the other hand, the deep outflows such as those from the Mediterranean and the Red Sea are dominated by bottom topography, that is, they belong to the second class of outflows, which is not the focus of our study (see, e.g., Killworth 1977; Johnson et al. 1994; Price and Baringer 1994; Condie 1995; Jiang and Garwood 1995; Jungclaus et al. 1995; Baringer and Price 1997a,b; Emms 1997, 1998; Etling et al. 2000).

River plumes that at times display at least some interaction with the bottom have beem studied by Garvine (1987, 1995, 1996), Csanady (1984), Chao and Boicourt (1986), Chao (1988), O'Donnell (1990), Münchow and Garvine (1993), Oey and Mellor (1993), Chapman and Lentz (1994), and Kourafalou et al. (1996). Most of these studies are numerical and show ballooning of the outflow near its origin, in line with some of the observations and with the PN nonsteadiness argument. A special case is that of a river entering the ocean at a small angle. Here, there is a very small momentum-flux deficit (proportional to the angle) and an approximate steady state can be reached (Garvine 1987, 2001; Horner et al. 2000).

Yankovsky and Chapman (1997) have attempted to develop an analytical bound on the inviscid size of the bottom-free bulges but their bound is inconsistent with the PN momentum-flux argument. This is due to their use of the upstream thickness as the bulge maximum thickness. As we shall see, there is no maximum bulge thickness.

c. Present approach

Consider the situation shown in Fig. 2. Our approach is to look at the bulge's growth process as a slowly varying problem. This is based on the idea that the process involves two timescales, one fast and one slow. The fast timescale [$O(f^{-1})$, where f is the Coriolis parameter] is associated with the time required for a particle to complete a single revolution within the gyre, whereas the slow timescale is the time associated with the gradual growth rate of the bulge. Namely, we shall focus on the time range where the bulge is already relatively large in the sense that its volume divided by the outflow mass flux gives a timescale much longer than a day. This is equivalent to saying that the bulge diameter (which is of the order of the Rossby radius based on the gyre's central depth) is much greater than the downstream current width. In this scenario, the bulge
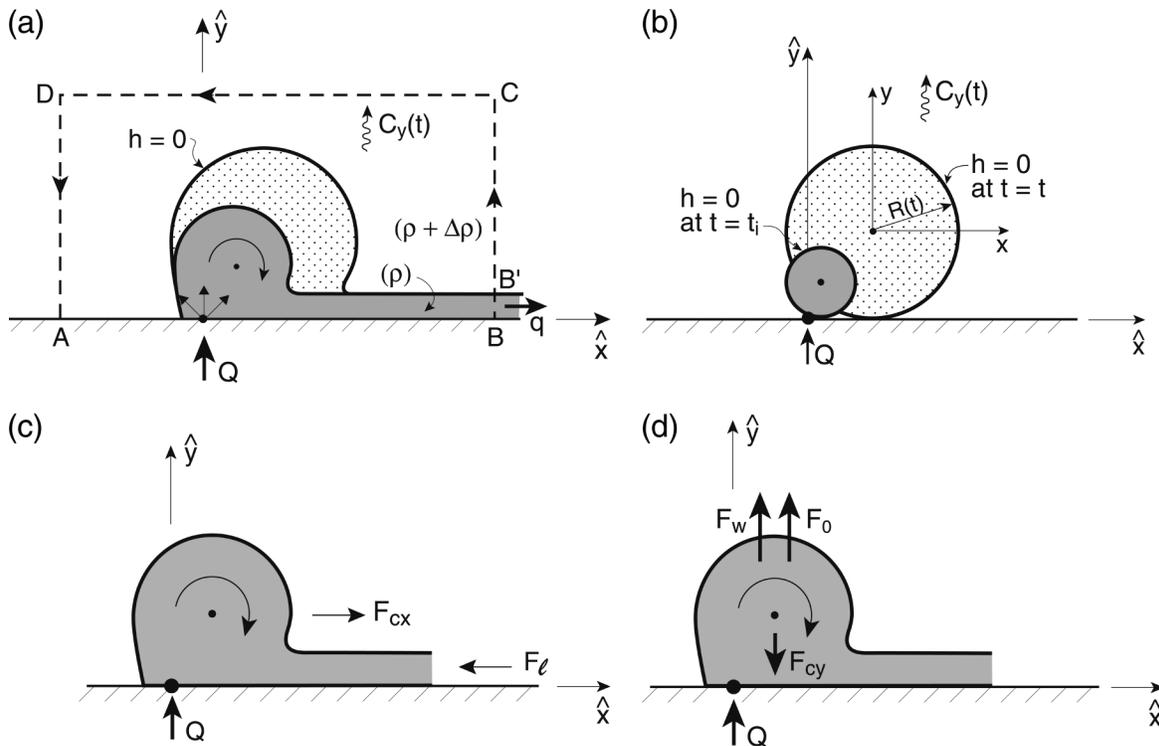
FIG. 2. (a) A schematic diagram of the model under study. The ''wiggly'' arrow indicates the off-wall and long-wall migration of the bulge $C_y(t)$; this results from the growth forcing the bulge itself away from the wall. The thick dashed line indicates the integration path that will be used. We focus on ''long'' time in the sense that the mass flux circulating within the bulge is already much greater than the outflow mass flux Q (and the downstream current mass flux q) so that the process is slowly varying in time. The (immiscible) layer densities are ρ and $(\rho + \Delta\rho)$. (b) The assumed (simplified) structure of the bulge basic state at $t = t_i$ and $t = t$; i.e., the axisymmetric state around which the (slowly varying) perturbation scheme is constructed. As shown, the bulge basic state circular edge is taken to be tangential (at all times) to the coast so that $C_y = dR/dt$. This plausible condition is justified because the gyre cannot grow unless it pushes itself away from the wall. (c) The balance of the long-wall forces acting on the outflow. The alongwall Coriolis force F_{cx} (resulting from the gyre's center migration in the y direction C_y) balances the momentum flux associated with the longshore current, F_l. (d) As in (c) but for the offshore forces. Here, the Coriolis force f_{cy} (resulting from the longshore migration) is pointing toward the wall. It is balanced by two forces. The first is the momentum flux associated with the source momentum flux F_0 (which, in contrast to the $\hat{x}$ component, does not vanish because the source is not symmetrical with respect to the $\hat{y}$ axis; i.e., the source velocity, v_s obeys $v_s(\hat{y}) \neq v_s(-\hat{y})$]. The second is the offshore pressure force associated with the nonzero thickness along the wall F_w. In contrast to the alongshore balance shown in (c) (which will be used in our calculation), this offshore balance cannot be used because of the impossibility of calculating F_w. It is shown here merely for completion.

growth rate is weak because the net mass flux into it $(Q - q)$ is small compared to the transport already circulating in it. (Note, however, that this slow growth accumulates over a long time to become an important effect.)

We shall first deal with an outflow that conserves its zero potential vorticity (PV) on both short and long timescales. Namely, we shall first look at the case where the zero PV is not only conserved at each moment but is also conserved over a long time. We shall then see that our slowly varying approach also allows for outflows whose PV is slowly altered in time. This is so because, just as the time derivative of the velocity and thickness are negligible (because they vary on the long timescale) so are the small frictional forces that cause the changes in the PV. That is to say, with our slowly varying approach, the potential vorticity is conserved on the short timescale (i.e., at each moment) but not

necessarily on the long timescale (i.e., from the beginning to the end). (We shall see that our numerical simulations clearly support this scenario.) In addition to the slowly varying approximation (which allows the neglect of all derivatives with respect to time in the governing equations), we shall also construct a perturbation scheme where the basic, undisturbed gyre is a circular gyre barely touching the wall (Fig. 2b).

Since the only simple analytical solution for a lenslike bulge on an f plane is the one for a zero PV bulge,[1] we shall initially limit ourselves to zero PV bulges. We shall later construct analytical solutions for bulges with (relative) anticyclonic vorticity smaller than f (correspond-

---

[1] Csanady (1979) derived an analytical solution for a finite potential vorticity lens, but the solution is not simple enough to be considered as a part of an involved perturbation expansion such as ours. Furthermore, it is inaccurate near the eddy's rim (Flierl 1979).

ing to nonuniform PV). The question of what happens when the incoming fluid has cyclonic rather than anticyclonic vorticity is not addressed here and is left as a subject of future investigation [but see Nof and Pichevin (1999)]. Strictly speaking, any (inviscid) finite PV outflow has a maximum gyre depth. However, since our PV is allowed to be gradually altered (via small frictional effects), such a limit does not exist in our case.

We consider the inviscid shallow-water equations in a coordinate system traveling slowly away from the wall with the gyre's center (section 2). We then consider the integrated balance of forces along the wall and neglect all terms of high order. After some fairly tedious algebra, we find a very simple analytical solution for the gyre's increase in size (section 3). It shows that the growth corresponds to a balance between the (long wall) momentum flux associated with the downstream current, and the compensating Coriolis force associated with the migration of the gyre center away from the wall.

Using a numerical "reduced gravity" model [of the Bleck and Boudra (1986) type] we then show (section 4) that, as the analytical solution predicts, the gyre's radius increases gradually. Encouraged by this, we then extend our analytical theory to the cases where the bulge's relative vorticity is smaller than f. The associated numerical simulations are also in very good agreement with this solution. They show that, even though the small frictional effects accumulate over time to alter the PV, the inviscid solution is valid *at each moment*. Possible applications of the theory to various outflows in the ocean are discussed, and the results are summarized in section 5.

2. Formulation

This section describes the physics of the problem and the mathematical approach. For clarity, the solution is presented in two stages. First, by skipping the stage associated with the establishment of the initial bulge and using the slowly varying process approach, we set all derivatives with respect to time to zero. We then introduce a streamfunction and construct a perturbation scheme where the zeroth-order state is a radially symmetric f-plane bulge. Because our problem involves a growing bulge, the usual procedure of formally nondimensionalizing all the terms at once and then performing an expansion is impossible. Instead, we shall retain the terms in dimensional form and examine their relative importance during each stage of the analysis.

The reader is warned in advance that it may be difficult to follow the mathematical analysis in detail. To alleviate some of this difficulty, it is useful to a priori introduce the governing equations that we are after. We are after two conservation relationships. The first is the (straightforward) integrated conservation of mass,

$$\frac{dV}{dt} = Q - q,$$

where $V(t)$ is the bulge volume (slowly varying in time), Q is the steady outflow mass flux, and q is the mass flux of the downstream current. The second relationship that we seek is the not-so-simple conservation of long-wall momentum flux (or flow force),

$$\int_S \int C_y fh \, dx \, dy = \int_B^C hu^2 \, dy$$

$$= \text{jet force due to downstream current},$$

where S is the bulge area, C_y the (slow) offshore migration of the bulge center (i.e., the point of maximum thickness), h the thickness, and u the downstream current speed. (Note that, for convenience, variables are defined both in the text and in appendix A.)

The term on the left is the long-wall Coriolis force created by the off-wall migration of the bulge center (Fig. 2b) resulting from the gyre growth (which forces it to push itself away from the wall). The term on the right is the momentum flux of the downstream flow (i.e., the force created by the ejection of mass from the control volume). This balance of forces along the wall is shown in Fig. 2c. In contrast to this balance, which plays a crucial role in our calculations, the complementary offshore balance of forces (shown in Fig. 2d) cannot be used because of the impossibility of computing the offshore pressure force; therefore, it will not be dealt with. This implies that C_x, the bulge's migration in the x direction, cannot be determined with our approach. With the above presentation of the main governing equations, the reader who is primarily interested in the results can now go directly to the solution (3.3)–(3.7).

We now begin the detailed derivation of the governing equations. First, as already mentioned, we note that the problem involves a "fast" timescale (i.e., days) and a "slow" timescale (i.e., weeks, months, or years). The fast timescale is associated with the (geostrophic) adjustment timescale and with the relatively short time that it takes a particle to complete a single revolution within the (zero PV) bulge. This fast time is also the time that it takes a particle to get from the gyre to the downstream current. By contrast, the slow timescale is associated with the slow offshore migration of the bulge center, which implies a large bulge radius compared to the downstream current scale. The conceptual small parameter of our problem is then the ratio between these short and long timescales or, equivalently, the ratio between the downstream mass flux q (or the incoming mass flux Q) and the mass flux circulating within the bulge. To see this more clearly, we note that the volume of the gyre at any arbitrarily long time T ($\gg f^{-1}$) is of the order of QT so that the mass flux circulating in it is $\sim O(QTf)$ and its radius [$\sim O(g'QT)^{1/4}/f^{1/2}$] is much greater than the downstream current width, which is of the order of $(g'Q)^{1/4}/f^{3/4}$. Namely, if we wait a long

enough time ($\gg f^{-1}$) after the outflow is first "turned on," then the size of the bulge is much greater than the downstream current.

In what follows we shall consider the detailed conservation of mass and momentum for the problem and examine the associated scales. We shall neglect all the time-dependent terms in the (differential) momentum and continuity equations a priori and, once the solution is obtained, show that they are indeed small compared to the smallest terms that were kept. This is the simplest way to present our analysis, as it is a simple matter to examine the smallness of the neglected terms once the analytical solution is obtained.

a. Conservation of mass

The integrated mass conservation equation can be written as

$$\frac{d}{dt} \int_S \int h \, dx \, dy = Q - q, \qquad (2.1)$$

where the left-hand side is the bulge's volume rate of change (which is very slow) and the right-hand side is the difference between the steady incoming mass flux Q and the outgoing transport of the longshore current q. As mentioned, since the time associated with the volume change is long, one immediately sees that the downstream current thickness is small compared to the thickness of the bulge and that its width is much smaller than the radius of the gyre.

b. Momentum flux

To examine the momentum-flux balance, we write all of the nonlinear momentum equations (multiplied by h) and the continuity equation in a coordinate system moving with the gyre's center away from the wall,

$$h\frac{\partial u}{\partial t} + h\frac{\partial C_x}{\partial t} + hu\frac{\partial u}{\partial x} + hv\frac{\partial u}{\partial y} - f(v + C_y)h$$

$$+ \frac{g'}{2}\frac{\partial}{\partial x}(h^2) = 0 \qquad (2.2a)$$

$$h\frac{\partial v}{\partial t} + h\frac{\partial C_y}{\partial t} + hu\frac{\partial v}{\partial x} + hv\frac{\partial v}{\partial y} - f(u + C_x)h$$

$$+ \frac{g'}{2}\frac{\partial}{\partial y}(h^2) = 0 \qquad (2.2b)$$

$$\frac{\partial h}{\partial t} + \frac{\partial}{\partial x}(hu) + \frac{\partial}{\partial y}(hv) = 0, \qquad (2.3)$$

where, as before, the conventional notation is given in both the text and in appendix A. Namely, u and v are the horizontal velocity components (in the moving coordinate system), C_x and C_y are the time-dependent migration rates in the x and y directions, g' is the reduced gravity, and t is time. Note that (2.2)–(2.3) were ob-

tained by applying the familiar transformation $y = \hat{y} - \int_0^{\hat{t}} C_y(t)\, d\hat{t}$; $x = \hat{x} - \int_0^{\hat{t}} C_x(t)\, d\hat{t}$; $t = \hat{t}$ (where the variables with carets are associated with the fixed coordinate system and the absence of a caret denotes the variables in the moving system) to the usual time-dependent equations.

Four comments should be made regarding (2.1)–(2.3). First, in the moving coordinate system the wall appears to be slowly moving away from the gyre so that the wall boundary condition is

$$v = -C_y \quad \text{at } y = y_{\text{wall}} - \int_0^t C_y \, dt.$$

This wall condition is given here merely for completeness. We shall see that, because of our slowly varying approximation, it will never enter the problem. Second, Eq. (2.2b) will not be used because it is impossible to calculate the pressure exerted on the outflow by the wall with the method that we shall use. Hence, C_x will not be computed and (2.2b) is given here merely for completeness.

Third, the condition $C_y = dR/dt$ (implying that the bulge's basic state is barely touching the wall at all times) will be used to close the problem. The condition is plausible because the gyre cannot grow unless it pushes itself away from the wall. A very similar condition was used by Nof (1999). We shall see later that it is clearly supported by the numerics. Fourth, as in PN and Nof and Pichevin (1999) and Nof (1988), we shall neglect the source contribution to the alongshore momentum flux. This is done on the grounds that, at the source, the velocities go to infinity so that the effect of rotation is negligible and, consequently, the source is symmetrical relative to the x axis [i.e., v_s, the speed at the source, obeys $v_s(\hat{x}) = v_s(-\hat{x})$] even in the presence of rotation (see, e.g., Nof 1988, his Fig. 4 and section 7). Alternatively, one can assume that the outflow is fed by a narrow channel containing streamlines parallel to the wall (see PN).

Recall that our approach is to look at the bulge growth process as a slowly varying problem (assuming that the process involves two timescales, one fast and one slow). The fast timescale [$O(f^{-1})$] reflects the orbital periodicity, whereas the slow timescale reflects the very gradual growth rate of the bulge. Namely, we shall focus on the time range where the bulge is already relatively large in the sense that its volume divided by the outflow mass flux gives a timescale much longer than a day; that is, we focus on periods much larger than $O(f^{-1})$. As mentioned, this is equivalent to stating that the bulge diameter is much greater than the downstream current width. In this scenario, the bulge growth rate is weak in the sense that is associated with a small net transport (into the bulge) compared to the transport already circulating inside the bulge.

In addition to the different times issue, we shall later assume that the bulge's shape is nearly circular at all

times. This near-circular approximation is analogous to that made in Nof and Pichevin (1999) and implies that a circular gyre barely touching the wall is the state around which the solution is perturbed. This may appear at first to be a crude approximation. We shall see later, however, that it is actually a fairly good one given our integration approach. As mentioned, in line with the slowly varying approximation, all terms that include derivatives with respect to time in both the momentum and continuity equations are neglected. After the solution is obtained, we shall show that the neglected terms are indeed small.

With these important simplifications, the x-momentum equation is now integrated over the area bounded by the thick dashed line shown in Fig. 2a, noting that, outside the gyre, $h \equiv 0$. Using the approximated continuity equation, one finds

$$\int_S \int \left[\frac{\partial}{\partial y}(huv) + \frac{\partial}{\partial x}(hu^2) \right] dx\, dy$$

$$- \int_S \int f(v + C_y)h\, dx\, dy$$

$$+ \frac{g'}{2} \int_S \int \frac{\partial}{\partial x}(h^2)\, dx\, dy = 0. \qquad (2.4)$$

Note that, since in our coordinate system the wall is moving slowly away from the gyre, the integration area S is a (weak) function of time. This movement of the wall has no direct bearing on our bulge momentum calculation because all of the time-dependent terms are ignored.

Next, we define the streamfunction ψ to be $\partial\psi/\partial y = -uh$, $\partial\psi/\partial x = vh$ and rewrite (2.4) as

$$\int_S \int \left[\frac{\partial}{\partial y}(huv) + \frac{\partial}{\partial x}(hu^2) \right] dx\, dy$$

$$- \int_S \int f\frac{\partial\psi}{\partial x}\, dx\, dy - \int_S \int C_y fh\, dx\, dy$$

$$+ \frac{g'}{2} \int_S \int \frac{\partial}{\partial x}(h^2)\, dx\, dy = 0. \qquad (2.5)$$

Application of Stokes' theorem (which, for our problem, is just a special case of Green's theorem) to (2.5) gives,

$$\oint_\phi huv\, dx - \oint_\phi (hu^2 + g'h/2 - f\psi)\, dy$$

$$+ C_y \int_S \int fh\, dx\, dy = 0, \qquad (2.6)$$

where ϕ is the boundary of S (i.e., ABCDA) and the arrowed circles indicate counterclockwise integration. With the exception of section BC (Fig. 2), at least one of the three variables h, u, and v vanish along the bound-

ary. Also, with the slowly varying approach, ψ can be taken to be a constant along the boundary.

In view of these, (2.6) can be written as

$$- \int_B^C \left(hu^2 + \frac{g'h}{2} - f\psi \right) dy + C_y \int_S \int hf\, dx\, dy = 0. \qquad (2.7)$$

Application of the Bernoulli principle to the front ($h = 0$) implies that the speed along the outer edge of the downstream current must be approximately equal to the orbital speed along the gyre periphery. However, both thickness and width of the downstream current are small compared to the thickness and radius of the bulge. Namely, within the downstream current $u \sim O(g'H)^{1/2}$ (where H is the *gyre's* depth scale) but $h \ll H$ and, hence, the last two terms within the first integral are small compared to the first and can be neglected. In view of this, (2.7) can be ultimately written as

$$- \int_B^C hu^2\, dy + C_y \int_S \int fh\, dx\, dy = 0. \qquad (2.8)$$

Equation (2.8) represents a balance of two longshore forces (Fig. 2c). The first is a long-wall force associated with the downstream current. It is analogous to the force produced by a jet. The second is an integrated Coriolis force resulting from the offshore migration of the gyre center. This migration results from the fact that the gyre is in constant contact with the wall so that by growing it pushes itself away from the wall.

When a similar treatment is given to (2.2b), one finds a balance between three offshore forces (Fig. 2d). Because of the impossibility to compute the offshore pressure force exerted on the outflow by the nonzero thickness along the wall, the balance will not be used and is mentioned here, in passing, merely for completion. Our inability to use (2.2b) implies that we will not be able to compute C_x with our approach.

3. Solution

To obtain the solution to the problem we now introduce the perturbation scheme,

$$u = \overline{u} + u' + \cdots; \qquad h = \overline{h} + h' + \cdots, \qquad (3.1)$$

where the overbars denote association with a radially symmetric f-plane bulge barely touching the wall (Fig. 2b) and the primes denote distortions introduced by the wall. This "small distortion approximation" is analogous to that used in Nof and Pichevin (1999). The introduction of this perturbation scheme implies that our problem is not only slowly varying in time but also that, at any given moment, the gyre shape is not very far from the circle shown schematically in Fig. 2b.

It is worth pointing out again at this stage of the presentation that, given our slowly varying approach, our gyre does not have to conserve potential vorticity

on the long timescale but must conserve potential vorticity *on the short timescale*. That is to say, at each moment in time, the gyre's potential vorticity must be equal to the downstream current's potential vorticity. However, frictional effects, which at each given moment are small and negligible, can accumulate over the long time period to become important and alter the PV. We shall return to this important aspect momentarily.

a. Approximated conservation of mass

By substituting (3.1) into (2.1) and keeping only the highest-order terms, we find

$$\frac{d}{dt} \iint \bar{h} \, dx \, dy = Q - q. \quad (3.2a)$$

Focusing, for the moment, on a zero PV outflow whose PV is not altered during the slow growth process we get

$$\frac{16\pi f^2 R_d^3}{g'} \frac{dR_d}{dt} = Q - q. \quad (3.2b)$$

In deriving (3.2b) it has been taken into account that the volume of a zero PV bulge is $4\pi f^2 R_d^4/g'$ [because $h = H(t) - f^2 r^2/8g'$ where $H(t)$ is the gyre's central depth (see, e.g., Nof 1981a,b)]. Here, R_d is the time-dependent Rossby radius, $[g'H(t)]^{1/2}/f$.

b. Approximated momentum flux

Substituting (3.1) into (2.8) and neglecting products of the perturbations (and keeping in mind that, although within the downstream current the speed is high, the width of the current is small), we get

$$-\int_0^L h'(\bar{u})^2 \, dy + C_y \iint_S f\bar{h} \, dx \, dy = 0, \quad (3.3a)$$

where $\bar{S}$ is the area that the basic bulge occupies (Fig. 2b), and L is the (small) downstream current width. Note that, along the bulge's edge, the velocity is $fR/2$ (where R is the bulge radius) so that the downstream current speed along the edge is also $\bar{u} = fR/2$. This is so because $h = 0$ along the edge so that the Bernoulli principle implies that the velocity along the edge of the bulge is the same as the velocity along the edge of the downstream current. Furthermore, since the downstream current is very narrow compared to the bulge, the shear across it can only produce small variations in the velocity and, consequently, our perturbation scheme implies that its velocity should be taken to be uniform across it (i.e., $\bar{u} = fR/2$ is the uniform speed for the downstream current). It is important to realize that this is also true for the nonzero PV case, that is, the velocity of the downstream current should be taken to be uniform even in the finite or variable PV case.

In view of this, one of the $\bar{u}$ constituting the square

of the velocity in the first integral of (3.3a) can be taken outside the integral, and (3.3a) can be rewritten as

$$-\frac{fRq}{2} - C_y \iint_{\bar{S}} f\bar{h} \, dx \, dy = 0, \quad (3.3b)$$

because $q = \int_0^L h'\bar{u} \, dy$.

Taking again into account the known velocity and depth profiles of a radially symmetric zero PV bulge, we find that, for a zero PV conserving gyre, (3.3b) takes the form

$$-\frac{\sqrt{2}g'q}{16\pi} + \sqrt{2}R_d^3 f \frac{dR_d}{dt} = 0. \quad (3.4)$$

Note that the condition $C_y = dR/dt$ has also been used. As already pointed out, the relationship $C_y = dR/dt$ involves the plausible assumption that the bulge progresses away from the wall at the same rate that its radius is increased; that is, it is forever in touch with the wall and pushes itself away from the wall as it grows.

c. Detailed solution

Elimination of q between (3.2b) and (3.4) gives a single differential equation for the instantaneous R_d,

$$-3R_d^3 f^2 \frac{dR_d}{dt} + \frac{g'Q}{8\pi} = 0.$$

The solution obeying the initial condition $R_d = R_{di}$ at $t = t_i$ is

$$R_d = \left[R_{di}^4 + \frac{g'Q(t - t_i)}{6\pi f^2} \right]^{1/4}. \quad (3.5)$$

Relation (3.5) implies that the instantaneous bulge central depth H is

$$H = \left[H_i + Q(t - t_i) \left(\frac{f^2}{6\pi g'} \right) \right]^{1/2}, \quad (3.6)$$

and that the bulge radius R is

$$R = \left[R_i^4 + \frac{32g'Q(t - t_i)}{3\pi f^2} \right]^{1/4}. \quad (3.7)$$

The speed that the gyre's center moves offshore is

$$C_y = \frac{8g'Q}{3\pi f^2 R^3}. \quad (3.8)$$

Finally, we find that two-thirds of the outflow's mass flux goes into the gyre and the remaining one-third goes into the downstream current. Recall that, in the above solution, the initial state (denoted with the subscript i) is not the state corresponding to the time that Q is first "turned on." Rather, it is associated with an arbitrary time corresponding to a bulge that is already much greater than the downstream current. It is of interest that, according to this solution, the mass fluxes into both the downstream current and the bulge are constants. Name-

ly, even though the bulge grows forever in size, its offshore migration decreases in such a manner that the mass flux into it is steady. Using our solution (3.5)–(3.8), it is now a trivial matter to show that all the time-dependent terms originally ignored in our slowly varying derivation (section 2) are indeed small and negligible. Furthermore, they all get smaller and smaller as time goes on, making our approximation better and better.

Using similar principles we can now derive the corresponding expressions for a bulge whose PV is not zero. Namely, we shall now consider a bulge whose PV is either nonzero to begin with or a bulge whose potential vorticity has been very gradually altered (by frictional processes) over a very long period of time. To do so, we consider a gyre whose mean (instantaneous) orbital flow $(\overline{v_\theta})$ is given by

$$\overline{v_\theta} = -\frac{\alpha f r}{2}, \qquad \alpha < 1, \tag{3.9}$$

so that its (instantaneous) volume V is $\alpha(2 - \alpha)\pi f^2 R^4/16g'$ and its radius is $R = 2\sqrt{2}R_d/\alpha^{1/2}(2 - \alpha)^{1/2}$. Note that, in general, this gyre does not correspond to a uniform PV outflow. [However, for $\alpha = 1$, (3.9) reduces to the familiar uniform zero PV case.] Note further that our governing equations (3.2a) and (3.3b) are still applicable because, with our perturbation scheme, the speed of the downstream current $fR/2$ is taken to be uniform across the current regardless of the gyre's PV. We find that the ratio of the mass flux going into the gyre and the incoming mass flux Q is

$$\frac{dV}{dt}\bigg/ Q = \frac{2\alpha}{(1 + 2\alpha)}, \tag{3.10}$$

and that the gyre growth rate dR/dt is

$$C_y = \frac{dR}{dt} = \frac{8g'Q}{\pi f^2 R^3(1 + 2\alpha)(2 - \alpha)}. \tag{3.11}$$

We also find

$$R = \left[R_i^4 + \frac{32g'Q(t - t_i)}{\pi f^2(1 + 2\alpha)(2 - \alpha)}\right]^{1/4} \tag{3.12}$$

$$H = \left[H_i^2 + \frac{f^2\alpha^2(2 - \alpha)Q(t - t_i)}{(1 + 2\alpha)2\pi g'}\right]^{1/2}, \tag{3.13}$$

which reduce to (3.7) and (3.6) for $\alpha = 1$, as should be the case. We see from (3.10) that, in the weak gyre case ($\alpha \ll 1$), most of the outflow's mass flux Q now goes into the downstream current rather than into the bulge.

4. Numerical simulations

To further analyze the validity of our assumptions (e.g., that the flow is parallel to the wall downstream), we shall now present numerical simulations and quantitatively analyze the results.

a. Numerical model description

We used a modified version of the Bleck and Boudra (1986) reduced-gravity isopycnic model with a passive lower layer and employed the Orlanski (1976) second-order radiation conditions for the open boundary. We found that this condition is satisfactory because the downstream streamlines were not disturbed when they crossed the boundary.

We performed several experiments with outflows whose *initial* PV is either zero or finite. The results of each experiment within a given group were very similar to each other and, consequently, we present here only one experiment of each group. Since each run provides numerous data points we believe that this presentation is adequate. As is typical for these kinds of experiments, our wall was slippery and we took the vorticity to be zero next to it. We began the experiment by turning on an outflow at $t = 0$; our numerical source was a channel containing streamlines parallel to the channel walls. The width of the channel was such that the thickness vanished along the left wall (looking downstream). The initial phase involved the initial establishment of the gyre, which could last up to several days.

Both runs that we present were conducted with a relatively high resolution corresponding to $\Delta x = \Delta y = 3.6$ km in a basin 360 km $\times$ 720 km. For numerical stability, we chose an eddy viscosity of 360 m^2 s^{-1}; the time step was 5 min and the upstream thickness along the channel's right bank was 450 m. Our mass flux was always 20 Sv and, as mentioned, we chose the channel width so that the thickness was zero along the left wall. We ran both the zero PV and the finite PV experiment for a long time (100 days) so that even the zero PV experiment ultimately had its potential vorticity altered by the cumulative effects of friction. This enabled us to obtain data for nonzero PV outflow even from the "zero PV" experiment. The above resolution choices were certainly adequate for our Rossby radius of 30 km (corresponding to $g' = 2 \times 10^{-2}$ m s^{-2}, $f = 10^{-4}$ s^{-1}, and $H = 450$ m). Furthermore, these choices always allowed for at least ten grid points across the downstream current, which is also adequate.

b. Results

The results are shown in Figs. 3–9. All show very good agreement with the theory despite the fact that the error in the perturbation expansion is relatively large [of $O(\varepsilon^2)$ where ε, the ratio between the downstream current width and the bulge radius, was roughly 0.4]. The reason for the relatively small deviations of the numerics from the analytics (despite the relatively large ε) is that the calculation is based on surface integrations,
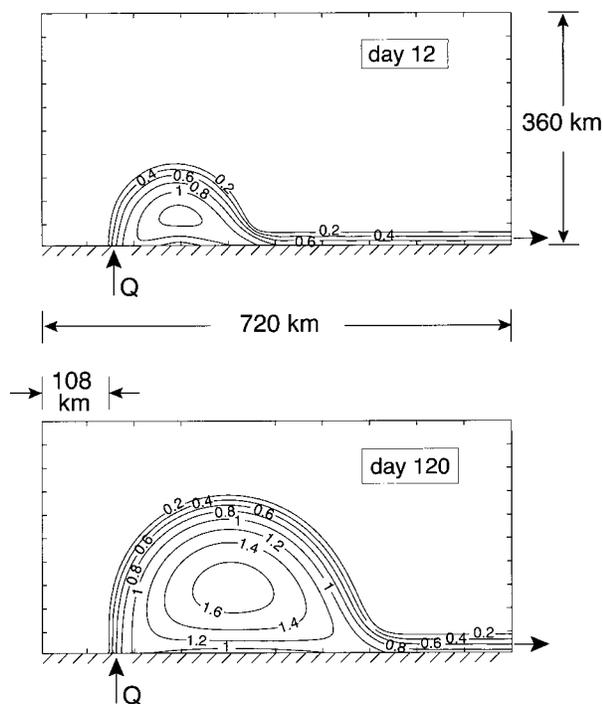
FIG. 3. Nondimensional thickness contours (h/Ĥ) for a zero PV outflow. Note that, as originally assumed (Fig. 2c), the gyre center moves both away from the wall and away from the source. It drifts approximately in the two o'clock direction away from the source. This migration is not exactly as we have assumed (1½ o'clock direction, corresponding to a 45° angle) because of the shape distortion. Physical constants: $f = 10^{-4}$ s^{-1}; $g' = 2 \times 10^{-2}$ m s^{-2}; $Q = 20$ Sv; $R_d = 30$ km; $\hat{H} = 450$ m; grid size $\Delta x = \Delta y = 3.6$ km; time step, $\Delta t = 5$ min; eddy viscosity, 360 m^2 s^{-1}.

which usually are not very sensitive to the gyre's shape because they smooth out the errors.

Figure 3 shows that, as the theory predicts, a gyre whose size increases in time is indeed established. The flow separates from the wall to the right of the source but this has no bearing on our solution even in the limit of no viscosity, which may involve velocity discontinuities because the equations that are used must still be satisfied. Figure 4 shows that, on the long timescale, the PV is (very gradually) altered by the small frictional forces. The alteration in time is greater in the zero PV case (upper panel) than in the finite PV case because the velocities and, hence, the frictional effects are larger. Since our slowly varying approach merely requires the PV to be conserved at each moment (i.e., on the *short* timescale), this small frictional effect that accumulates over the long time to become important does not invalidate the theory.

Figure 5 is the "backbone" of our analytical–numerical comparison as it shows a comparison of the two most important numerical momentum fluxes as a function of time. We see that, although the fluxes vary with time, at each moment, the integrated Coriolis force (resulting from the offshore migration) balances the down-
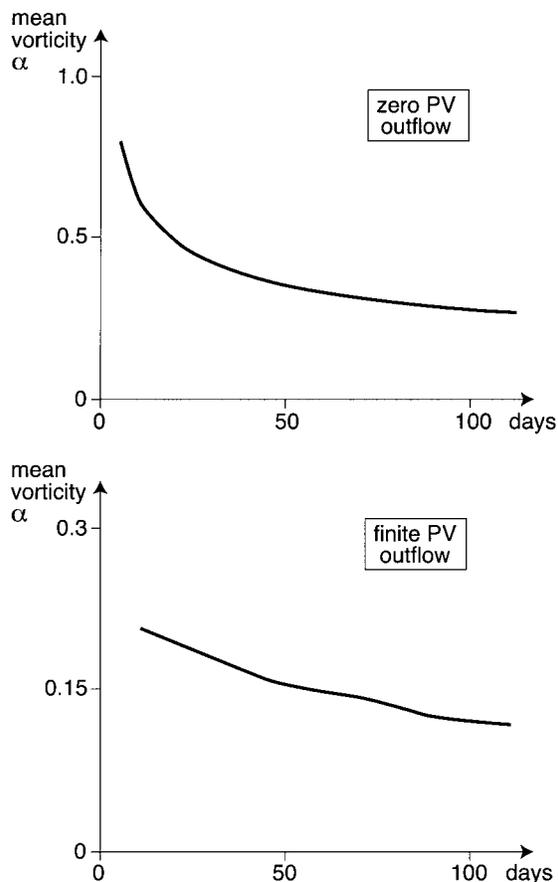

FIG. 4. The nondimensional mean vorticity (averaged over the gyre) as a function of time. The parameter α is the relative vorticity nondimensionalized with the Coriolis parameter. Note that, due to the length of our integration and the accumulative effect of (small) frictional effects, the mean vorticity decreases significantly even in the zero PV outflow case (upper panel). The reduction is less dramatic in the finite PV case (lower panel) because the initial velocities are smaller so that the frictional forces are smaller too. (The finite PV outflow case corresponds to a PV depth of 500 m, i.e., an upstream relative vorticity of $0.1f$ near the right bank.)

stream momentum flux, as (2.8) and (3.3a) imply. Namely, it illustrates that there are no unaccounted forces and that, despite the fact that frictional effects accumulate over time to become an important effect, at each moment in time the inviscid balance of forces is a valid approximation to the problem.

Figure 6 shows a comparison of the analytical and numerical mass fluxes for the zero and finite PV outflows. We see that the strict zero PV solution (dashed line in upper panel) is really never in good agreement with the numerics because it is supposed to hold only in the very beginning of the experiment at, say, $t < 5$ days (before the PV has been altered by friction) but in this short time the gyre is not yet well established. After this time, the PV is already altered so the altered solution [solid line corresponding to (3.10)] applies. Again we see that the agreement is better in the finite PV case
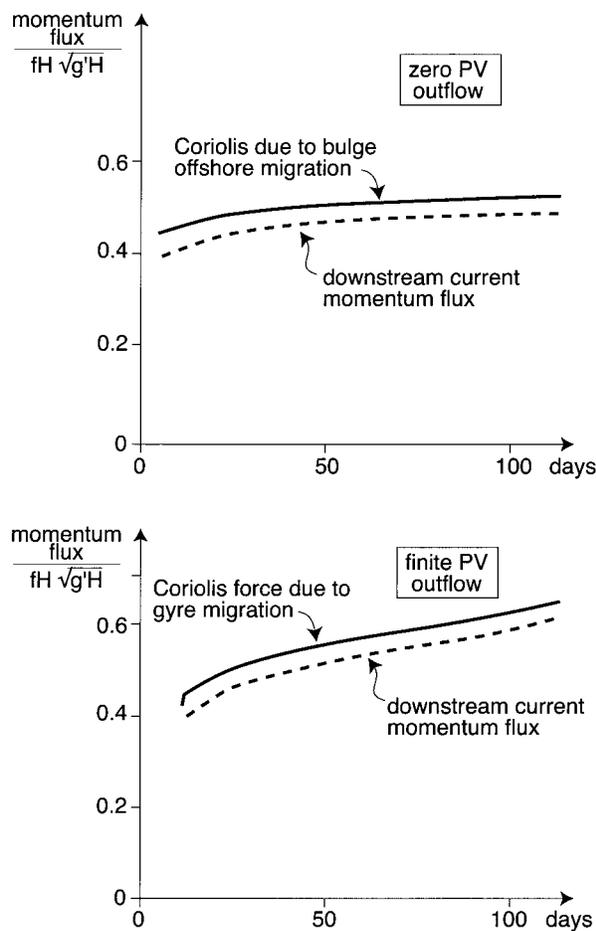
FIG. 5. A comparison of the (numerical) downstream current momentum flux (dashed line) to the (numerical) Coriolis force associated with the growth of the gyre and the resulting movement of its center away from the wall (solid line). It is clear that, at all times, the two are almost the same, in excellent agreement with our inviscid analytical derivation (2.8) and the "slowly varying" assumption.
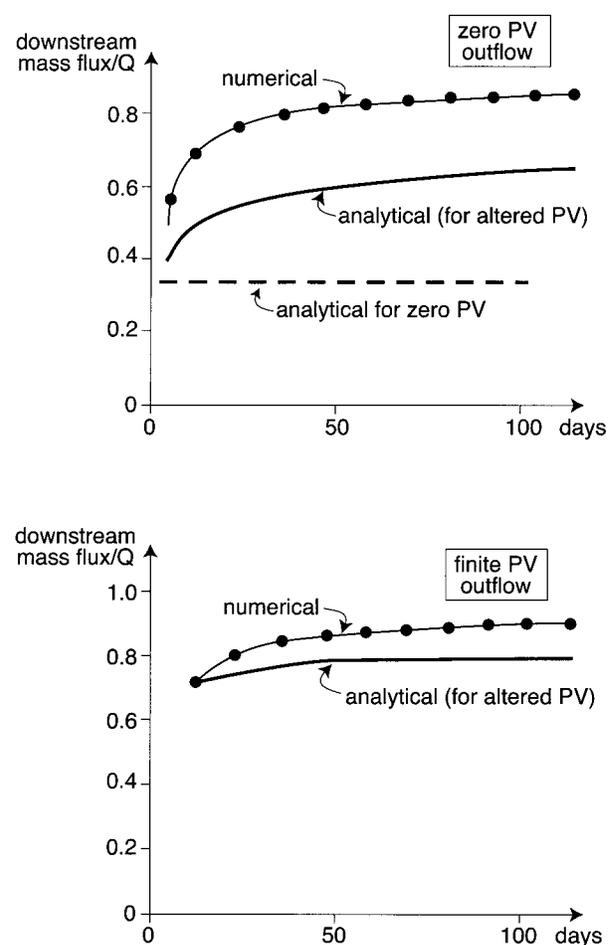
FIG. 6. The ratio of the downstream current mass flux to the incoming mass flux as a function of time. Note that, in the intense outflow case (i.e., zero PV), most of the initial mass flux goes to the bulge. After a while, the opposite is true and most of the flux goes to the downstream current. This is due to the reduction in vorticity (see text). The difference between the numerics and the analytics is primarily due to the frictional forces, which, as expected, are higher in the intense-outflow case because of the associated higher speeds. The dashed line in the upper panel represents the analytical solution for a zero PV bulge ($\alpha = 1$). Since the PV is gradually altered (on the long timescale), we also present an analytical solution based on the numerically observed vorticity shown earlier in Fig. 4. This is shown by the thick solid line.

because the frictional effects are smaller. The same can be said of the gyre volume (Fig. 7), the mean radius (Fig. 8), and the maximum depth (Fig. 9).

We also ran an experiment (not shown) where we doubled the eddy viscosity. We found that the mass flux of the downstream current *increased*. That is, the frictional effect (which causes an increased downstream current) explains why the theoretical volume increases more *rapidly* than the actual numerical values (Fig. 7). The results of the second set of experiments (weak, finite PV outflow) are in better agreement with the numerics than the zero potential vorticity case because the velocities are smaller so that the frictional forces are smaller too.

c. Limitations

As is frequently the case, both the analytical and the numerical model have their limitations. The three most

important weaknesses of the analytical solution result from the slowly varying assumption, the fact that we did not find the complete first-order solution, and the use of a 1½-layer model. (Note that the latter limitation is also present in the numerics.) We shall take these three issues one by one.

The first assumption eliminates the contribution of the time-dependent terms to the alongshore momentum flux. The assumption has been used successfully before and is valid as long as the bulge is much larger than the downstream current. The second limitation can be important because the complete first-order solution may impose constraints that may restrict the validity of our
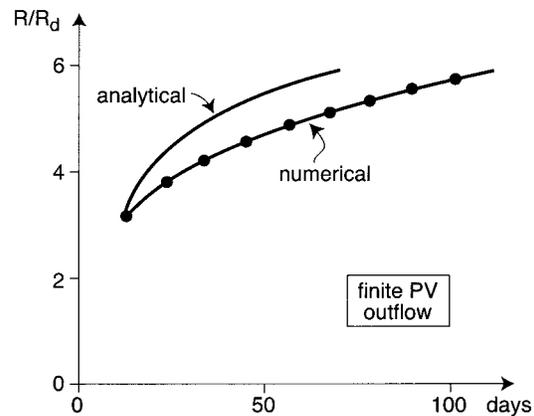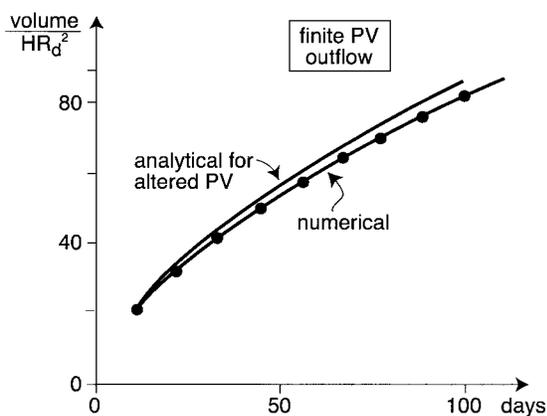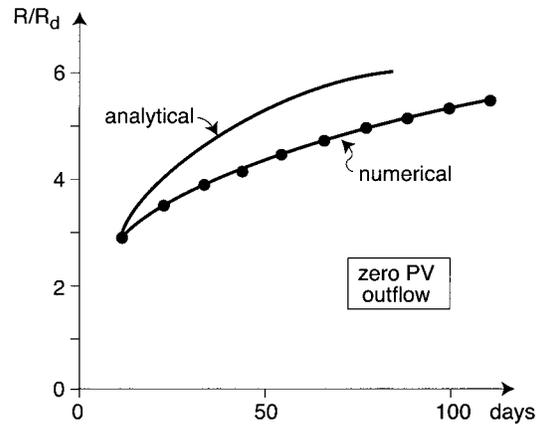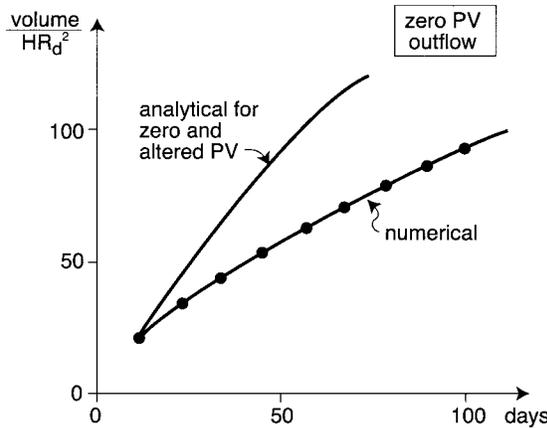
FIG. 7. A comparison of the numerical and analytical values for the volume of the bulge as a function of time. As before, the analytical calculations are based on a relative vorticity that is altered in time (Fig. 4). Since the errors shown in Fig. 6 accumulate over time, the discrepancy between the analytical and the numerical volumes increases with time.

FIG. 8. The mean radius of the bulge [defined by the square root of the area occupied by the bulge (up to the point where the curvature reaches a minimum, i.e., the streamlines become parallel to the wall) divided by π] as a function of time. As before, the analytical solution is based on the altered relative vorticity (Fig. 4).

solution. Our third limitation (resulting from the 1½-layer approach) excludes baroclinic instabilities (of both the bulge and the downstream current) and prevents the bulge from radiating energy outward. This essentially eliminates a nonfrictional decay from the problem.

5. Discussion and summary

The foregoing theory is applicable to various situations because almost all bodies of water are connected to each other. We assumed that the inviscid bulge involves two timescales, a *fast* timescale (i.e., the orbital timescale) and a *slow* timescale (i.e., the time associated with its growth and the resulting offshore displacement of its center). Alternatively, the problem can be thought of as involving two speeds, a fast orbital speed (of the fluid within the bulge) and a slow offshore migration of the (growing) bulge center.

The results of our theory can be summarized as follows:

1) The general analytical solution [(3.10)–(3.13)] corresponds to a balance between two alongshore forces, the momentum flux resulting from the downstream current and the integrated Coriolis force resulting from the offshore movement of the bulge center (Fig. 2). The nonlinear analytical solution shows that the bulge volume, radius, and central depth all gradually increase (see Figs. 3–9).

2) Intense outflows (i.e., zero PV) are associated with a relatively rapid growing bulge where 66% of the outflow mass flux Q goes into the bulge and the remaining 33% goes into the downstream current. Weaker outflows [i.e., small relative vorticity ($\alpha f/2$, where $\alpha \ll 1$) bulges], on the other hand, display the opposite kind of behavior. Here, most of the mass flux $Q/(1 + 2\alpha)$ goes to the downstream current and a smaller fraction $2\alpha Q/(1 + 2\alpha)$ goes into the bulge.
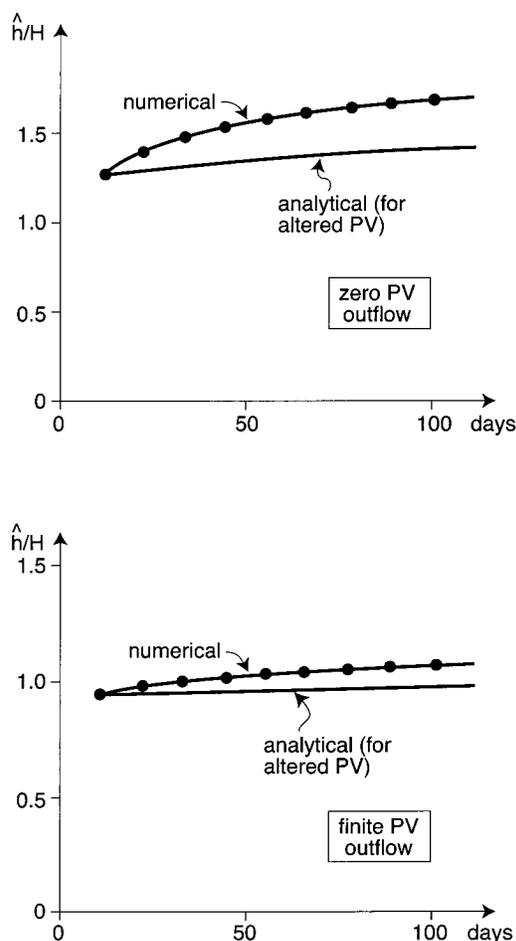
FIG. 9. The maximum thickness of the bulge as a function of time. Again, the analytical solution (3.13) is based on the altered relative vorticity shown in Fig. 4.

3) The numerical simulations illustrate that the balance of the two forces associated with the analytical solution is indeed valid (Fig. 5). Although the small frictional effects accumulate over time and change the potential vorticity, our most general inviscid solution [(3.10)–(3.13)] is a valid approximation to the instantaneous structure (Figs. 6–9).

Our results can be applied to various oceanic situations. For instance, the flow via the Yucatan Strait (in the initial Loop Current ring growth phase) can be viewed as our f-plane outflow problem. To see this, recall that PN argued that the associated Loop Current rings are generated to offset the downstream current momentum flux. They showed that β is responsible for the ultimate detachment of the rings and calculated their generation periodicity to be roughly 300 days. For periods shorter than 300 days, however, one can argue that β is perhaps not so important yet so that our present theory is applicable. Taking the incoming mass flux Q to be approximately 30 Sv, the radius of the rings to be 300 km, their depth to be 1000 m, and the incoming

inflow shear to be approximately $-f$ (see, e.g., PN), we find that 20 Sv would go into the initial buildup of the ring so that it would take approximately 100 days or so for a ring to reach a mature state.

In the above scenario, the next 200 days are used merely for β to take over the ring and force it to detach. Namely, the ring grows relatively quickly (within 3 months) but takes a long time to detach. Also, note that during the calculated 100 ring-growth days, the modeled downstream current carries merely 10 Sv because most (66%) of the water coming from the Caribbean enters the ring. On this basis, one would expect to find that the ring's growth process is associated with Florida Current transport fluctuations. Such changes have not, however, been observed (see, e.g., Maul and Vukovich 1993), probably because the Gulf of Mexico is closed. A closed basin means that the water that enters into the ring must somehow force other (lower layer) water to find its way out of the basin. Presumably, some of this advected water goes through the deep Yucatan Passage back into the Caribbean, but most finds its way into the Florida Current.

Another important application is to the period that it takes to establish the Tsugaru gyre. Recently, Nof and Pichevin (1999) have argued that the size of this gyre is determined by β, which arrests the gyre's growth. Again, one can perhaps argue that in the early stages of the gyre's establishment, β is not yet important so that the f-plane approximation may be adequate. Taking Q to be 1 Sv, the gyre radius to be 80 km, the reduced gravity to be 1.5×10^{-2} m s^{-2}, and the incoming vorticity to have the (admittedly large) value of $-f$, one finds that it would take about 180 days to establish the gyre. This is in agreement with the observations (see, e.g., Conlon 1982; Yasuda et al. 1988).

Going down in scale to outflows from rivers (such as the Mississippi) we find that for $f = 10^{-4}$ s^{-1}, a discharge of 10 000 m^3 s^{-1}, a reduced gravity of 2×10^{-2} m s^{-2} and a frictionally induced incoming vorticity of, say, $-0.05f$, about 80% of the discharge goes into the downstream current and about 20% into the bulge. Within a period of 100 days or so a bulge with a radius of 25 km will be formed.

An important question left unanswered is how can we a priori determine the vorticity of the bulge. In the large outflow case with an incoming anticyclonic vorticity, the potential vorticity is conserved and we do not have to worry about this issue. However, in cases where the vorticity of the incoming fluid is cyclonic rather than anticyclonic and in the small outflow case, the fluid must generate an anticyclonic vorticity on its own (via friction) so that a bulge is established. [Recall that this is indeed the case as shown numerically by both PN and Nof and Pichevin (1999).] How we can a priori calculate the vorticity that will be generated in these cases is not at all obvious.

APPENDIX

Definitions of Variables

C_x	alongshore migration of the bulge center
C_y	offshore migration of the bulge center
f	Coriolis parameter
g'	reduced gravity
H	bulge maximum thickness
$\hat{H}$	nondimensionalization thickness based on the upstream flow
h	thickness
h_B	thickness of the longshore current along the wall
L	downstream current width
q	mass flux via the downstream current
Q	outflow mass flux
R	bulge radius
S	bulge area
t	time
u, v	horizontal velocity components
V	bulge volume
v_θ	mean orbital flow of a gyre
α	relative vorticity nondimensionalized with the Coriolis parameter
ϕ	boundary of bulge area S
ψ	streamfunction (defined by $\partial\psi/\partial y = -uh$; $\partial\psi/\partial x = vh$)

REFERENCES

Atkinson, L. P., and D. Wallace, 1975: The source of unusually low surface salinities in the Gulf Stream off Georgia. *Deep-Sea Res.,* **23,** 913–916.

Baringer, M. O., and J. F. Price, 1997a: Mixing and spreading of the Mediterranean outflow. *J. Phys. Oceanogr.,* **27,** 1654–1677.

——, and ——, 1997b: Momentum and energy balance of the Mediterranean outflow. *J. Phys. Oceanogr.,* **27,** 1678–1692.

Bleck, R., and D. Boudra, 1986: Wind-driven spin-up in eddy-resolving ocean models formulated in isopycnic and isobaric coordinates. *J. Geophys. Res.,* **91,** 7611–7621.

Boicourt, W. C., 1973: The circulation of water on the continental shelf from Chesapeake Bay to Cape Hatteras. Ph.D. thesis, The Johns Hopkins University, 183 pp.

Bowman, M. J., 1978: Spreading and mixing of the Hudson River effluent into the New York Bight. *Hydrodynamics of Estuaries and Fjords,* J. C. J. Nihoul, Ed., Elsevier, 373–386.

Chao, S.-Y., 1988: River-forced estuarine plumes. *J. Phys. Oceanogr.,* **18,** 72–88.

——, and B. Boicourt, 1986: Onset of estuarine plumes. *J. Phys. Oceanogr.,* **16,** 2137–2149.

Chapman, D. C., and S. J. Lentz, 1994: Trapping of a coastal density front by the bottom boundary layer. *J. Phys. Oceanogr.,* **24,** 1464–1479.

Condie, S. A., 1995: Descent of dense water masses along continental slopes. *J. Mar. Res.,* **53,** 865–928.

Conlon, D. M., 1982: On the outflow modes of the Tsugaru warm current. *La Mer,* **20,** 60–64.

Csanady, G. T., 1979: The birth and death of a warm-core ring. *J. Geophys. Res.,* **84,** 777–780.

——, 1984: Circulation induced by river inflow in well mixed water over a sloping continental shelf. *J. Phys. Oceanogr.,* **14,** 1703–1711.

Drinkwater, K. F., 1988: On the mean and tidal currents in Hudson Strait. *Atmos.–Ocean,* **26,** 252–266.

Emms, P. W., 1997: Streamtube models of gravity currents in the ocean. *Deep-Sea Res.,* **44,** 1575–1610.

——, 1998: A streamtube model of rotating turbidity currents. *J. Mar. Res.,* **56,** 41–74.

Etling, D., F. Gelhardt, U. Schrader, F. Brennecke, G. Kühm, G. Chabert d'Hieres, and H. Didelle, 2000: Experiments with density currents on a sloping bottom in a rotating fluid. *Dyn. Atmos. Oceans,* **31,** 139–164.

Flierl, G., 1979: A simple model of the structure of warm- and cold-core rings. *J. Geophys. Res.,* **84,** 78–85.

Fong, D. A., 1998: Dynamics of freshwater plumes: Observations and numerical modelling of the wind-forced response and alongshore freshwater transport. Ph.D. thesis, Woods Hole Oceanographic Institution/Massachusetts Institute of Technology, 172 pp.

Garvine, R. W., 1987: Estuary plumes and fronts in shelf waters: A layer model. *J. Phys. Oceanogr.,* **17,** 1877–1896.

——, 1995: A dynamical system for classifying buoyant coastal discharges. *Contin. Shelf Res.,* **15,** 1585–1596.

——, 1996: Buoyant discharge on the inner continental shelf: A frontal model. *J. Mar. Res.,* **54,** 1–33.

——, 2001: The impact of model configuration in studies of buoyant coastal discharge. *J. Mar. Res.,* **59,** 193–225.

Horner, A. R., D. A. Fong, J. R. Koseff, T. Maxworthy, and S. G. Monismith, 2000: The control of coastal current transport. *Proc. Fifth Int. Symp. on Stratified Flow,* Vancouver, British Columbia, Canada, International Association of Hydraulic Research, 865–870.

Hurlburt, H. E., and J. D. Thompson, 1980: A numerical study of Loop Current intrusions and eddy shedding. *J. Phys. Oceanogr.,* **10,** 1611–1651.

Jiang, L., and R. W. Garwood Jr., 1995: A numerical study of three dimensional dense bottom plumes on a Southern Ocean continental slope. *J. Geophys. Res.,* **100,** 18 471–18 488.

Johnson, G. C., T. B. Sanford, and M. O. Baringer, 1994: Stress on the Mediterranean outflow plume. Part I: Velocity and water property measurements. *J. Phys. Oceanogr.,* **24,** 2072–2083.

Jungclaus, J. H., J. O. Backhaus, and H. Fohrmann, 1995: Outflow of dense water from the Storfjord in Svalbard: A numerical model study. *J. Geophys. Res.,* **100,** 24 719–24 728.

Killworth, P. D., 1977: Mixing on the Weddell Sea continental slope. *Deep-Sea Res.,* **24,** 427–448.

Kourafalou, V. K., L.-Y. Oey, J. D. Wang, and T. N. Lee, 1996: The fate of river discharge on the continental shelf. 1. Modeling the river plume and the inner shelf coastal current. *J. Geophys. Res.,* **101,** 3415–3434.

Masse, A. K., and C. R. Murthy, 1992: Analysis of the Niagara River plume dynamics. *J. Geophys. Res.,* **97,** 2403–2420.

Maul, G. A., and F. M. Vukovich, 1993: The relationship between variations in the Gulf of Mexico Loop Current and Straits of Florida volume transport. *J. Phys. Oceanogr.,* **23,** 785–796.

Münchow, A., and R. W. Garvine, 1993: Dynamical properties of a buoyancy-driven coastal current. *J. Geophys. Res.,* **98,** 14 025–14 031.

Nof, D., 1981a: On the β-induced movement of isolated baroclinic eddies. *J. Phys. Oceanogr.,* **11,** 1662–1672.

——, 1981b: On the dynamics of equatorial outflows with application to the Amazon's basin. *J. Mar. Res.,* **39,** 1–29.

——, 1988: Outflows dynamics. *Geophys. Astrophys. Fluid Dyn.,* **40,** 165–193.

——, 1999: Strange encounters of eddies with walls. *J. Mar. Res.,* **57,** 1–24.

——, and T. Pichevin, 1999: The establishment of the Tsugaru and the Alboran gyres. *J. Phys. Oceanogr.,* **29,** 39–54.

O'Donnell, J., 1990: The formation and fate of a river plume: A numerical model. *J. Phys. Oceanogr.,* **20,** 551–569.

Oey, L.-Y., and G. L. Mellor, 1993: Subtidal variability of estuarine outflow, plume, and coastal current: A model study. *J. Phys. Oceanogr.,* **23,** 164–171.

Orlanski, I., 1976: A simple boundary condition for unbounded hyperbolic flows. *J. Comput. Phys.,* **21,** 251–269.

Pichevin, T., and D. Nof, 1997: The momentum imbalance paradox. *Tellus,* **49,** 298–319.

Price, J. F., and M. O. Baringer, 1994: Outflows and deep water production by marginal seas. *Progress in Oceanography*, Vol. 33, Pergamon, 161–200.

Sturges, W., 1994: The frequency of ring separations from the Loop Current. *J. Phys. Oceanogr.,* **24,** 1647–1651.

Yankovsky, A. E., and D. C. Chapman, 1997: A simple theory for the fate of buoyant coastal discharges. *J. Phys. Oceanogr.,* **27,** 1386–1401.

Yasuda, I., K. Okuda, M. Hirai, Y. Ogawa, H. Kudoh, S. Fukushima, and K. Mizuno, 1988: Short-term variations of the Tsugaru Warm Current in autumn (in Japanese with English abstract and captions). *Bull. Tohuku Reg. Fish. Res. Lab.,* **50,** 153–191.